Inherent Structures in the NaCl−CsCl System at the Boundary between Crystallization and Glass Formation†

James W. Palko‡,§ and John Kieffer*,‡

Department of Materials Science and Engineering, University of Michigan, Ann Arbor, Michigan 48109, and Department of Materials Science and Engineering, University of Illinois, Urbana-Champaign, Illinois 61801

Received: July 12, 2004; In Final Form: October 5, 2004

Inherent structures give insight into the structural changes that accompany the glass transition. Here, we present data on the energetics and configurations of inherent structures for various compositions in the NaCl−CsCl system, which are dominated by long-range ionic interactions. By choosing these compositions so as to achieve both crystallization and glass formation for a given system, the two types of structural developments can be contrasted. We evaluate the glass formation process for systems cooled at constant pressure on the basis of the temperature dependence of the inherent structure energies and inherent structure pressures. We find a minimum in the pressure−volume relation for the inherent structures obtained for isobarically cooled configurations, which closely tracks the glass transition of the simulated system. We also compare the inherent structure energies resulting from cooling under constant-volume conditions with those resulting from constant-pressure cooling. The pressure−volume work integrated along the inherent structure $P-V$ curve is found to largely account for the differences between isobaric and isochoric inherent structure energies.

1. Introduction

The concept of inherent structure was introduced by Stillinger and Weber as a means to separate the vibrational and configurational contributions to the structural disorder that characterizes liquids and glasses.[1] In practice, this idea can be easily realized in molecular dynamics (MD) simulations of such systems. By abruptly removing all thermal energy from the simulated system at a given point along its phase space trajectory, the system settles into the configuration that corresponds to the closest local potential energy minimum. This configuration is called the inherent structure (IS) at that state point and represents the "cleanest" structural representation of an amorphous material; that is, it is freed of any thermal fluctuations that displace the system from a mechanically stable configuration.

When quenched from different points along a phase space trajectory, the system may end up in different energy minima, thus allowing one to map out a part of the potential energy landscape. This procedure has therefore been extensively used to gain information about the energy landscape of model glass formers,[2−5] which is perceived to be a convenient conceptual framework for examining structural relaxations associated with the glass transition.

One fascinating observation is the marked drop in the inherent structure energy, e_{IS}, that can be accessed by the system in the supercooled liquid regime before going through the glass transition.[6,7] At high temperatures, well within the liquid regime of the system, the average e_{IS} plateaus near an asymptotic high-temperature value. Upon cooling, there is at first little temperature dependence of the average e_{IS}. When approaching the glass transition, the e_{IS} value markedly decreases and reaches a new low-temperature plateau characteristic of the glassy state. The magnitude of the glass e_{IS} value depends on the cooling rate. When cooled under isochoric conditions, the plot of e_{IS} versus the temperature at which the system was equilibrated assumes an asymmetric sigmoidal shape,[6,7] with its inflection point well within the supercooled liquid regime and close to the glass transition temperature.

The inherent structure concept has been applied to a large range of systems.[8−10] The best-studied systems in this context, however, are binary mixtures of particles interacting via a short-ranged Lennard-Jones potential, where the radii of the two species are chosen sufficiently different for the mixture to consistently form a glass on MD time scales (e.g., refs 6, 11, and 12). Moreover, cooling of the systems in these studies typically takes place under constant-volume conditions. While both the effects of pressure and temperature changes on inherent structures and related properties have been examined,[13] investigations of glass-forming systems that in simulations have been cooled along a constant-pressure path, as it would occur in experiments, are relatively scarce.[14,15]

Here, we apply inherent structure analysis to mixtures of NaCl−CsCl, which expands the gamut of glass-forming systems studied in this way with regard to three aspects: (i) The ionic character of the constituents results in highly selective nearest-neighbor coordination, a type of order that prevails in the liquid state. Conversely, the long-range nature of Coulombic interactions causes the local packing of ions to be affected by the configuration of more distant neighbors. The contribution from many neighbors is likely to have an averaging effect, suppressing strong local fluctuations. We may therefore expect the energy landscape to be relatively uniform. While the inherent structures of glass formers that exhibit mixed covalent−ionic bonding and whose behavior is strongly influenced by Coulombic forces (e.g., silica and water) have been investigated (e.g., refs 8 and 15−19), and those of ionic systems in the liquid and crystalline states have been investigated as well (e.g., refs 20 and 21), apparently

† Part of the special issue "Frank H. Stillinger Festschrift".

* Corresponding author. E-mail: kieffer@umich.edu. Phone: (734) 763-5671. Fax: (734) 763-4788.

‡ University of Michigan.

§ University of Illinois.

10.1021/jp046930c CCC: $27.50
Published on Web 11/23/2004

purely ionic glasses have not yet been studied. (ii) Depending on the composition of the pseudobinary system, it potentially crystallizes. Single-component alkali halides are extremely poor glass formers. In fact, in our simulations, we were never able to prevent crystallization in pure NaCl. Only through addition of CsCl does the system become frustrated and retain an amorphous structure upon cooling. By choosing a composition at the boundary between crystallization and glass formation, we are able to achieve relatively well-relaxed structures by MD standards, even if they end up forming a glass. (iii) Cooling along an isobar more closely matches the glass-forming process in experiments. Equilibrating the liquids under zero-pressure conditions invariably results in inherent structures subject to tensile hydrostatic stress (since inherent structure quenches are done isochorically), and this should be expected if real liquids and glasses were quenched to their inherent structures. The higher the equilibration temperature, the more a structure would like to contract during the quench, and the more tensile the stress in the resulting inherent structure. This is particularly important for the molten salt systems studied here, because of their large coefficient of thermal expansion. Eventually, however, one should reach the tensile limit of the structure, and the temperature at which this occurs may be meaningful as a stability criterion for the material.

2. Procedural Details

2.1. Choice of System. Many inorganic glass formers exhibit mixed covalent−ionic bonding, which leads to the formation of networked structures and significant intermediate-range order. MD simulations are limited to short time scales, which adversely affects the study of solidification by precluding adequate structural relaxation. The extremely high cooling rates ($\sim 10^{12}$ K/s) can lead to glass formation in systems that would otherwise crystallize; likewise, it is difficult to show that the actual room temperature structure of true glass formers is achieved in simulations. This is an issue particularly for networked glasses where structural relaxation upon cooling involves significant reconfiguration in the bonding structure. We therefore chose pseudobinary mixtures in the NaCl−CsCl system as model glass formers for this study. Interactions in this system are almost purely ionic, allowing one to eliminate the need to account for covalent bonds.

2.2. Computational Methods. The systems studied consisted of 512 atoms of NaCl doped with CsCl in concentrations ranging from 0 to 15 mol %. Atomic interactions were modeled using an electrostatic/Born−Mayer form for the potential energy, ϕ, (eq 1).[22]

$$\phi = \sum_{i<j} C\frac{q_i q_j}{r_{ij}} + A_{ij}e^{-r_{ij}/\rho_{ij}}; \quad A_{ij} = 0 \quad r_{ij} \geq r_{\mathrm{BMcutoff}} \qquad (1)$$

C is the Coulomb constant, q_i is the charge on particle i, and r_{ij} is the distance between particles i and j. A_{ij} and ρ_{ij} are parameters of the Born−Mayer repulsion; in units of kilocalories per mole and nanometers, respectively, their values are $A_{\mathrm{Na-Na}} = 19\,207.32$, $A_{\mathrm{Na-Cl}} = 48\,445.14$, $A_{\mathrm{Na-Cs}} = 102\,633.61$, $A_{\mathrm{Cl-Cl}} = 114\,552.57$, $A_{\mathrm{Cl-Cs}} = 159\,919\,027.3$, $A_{\mathrm{Cs-Cs}} = 548\,418.81$, $\rho_{\mathrm{Cs-Cl}} = 0.018\,58$, and $\rho_{\mathrm{X-X}} = 0.029\,00$ for all other combinations. r_{BMcutoff} is the range of the repulsive interaction and is equal to half the side of the simulation box ($\sim$1.2 nm). These specific values for the potential parameters are based on a genetic algorithm optimization by Reardon.[23,24] The ions were assigned their full charges ($q_{\mathrm{cation}} = 1$, $q_{\mathrm{anion}} = -1$). Full periodic boundary conditions were applied to the cell, and long-range electrostatic contributions were calculated using the Ewald method. Molecular dynamics trajectories were calculated using a standard leapfrog Verlet integration scheme with a time step of 2 fs. Temperature was controlled using velocity rescaling. To examine any change in inherent structures with temperature, the systems were cooled from temperatures well above the melting point (1300 or 1700 K) to well below the glass transition/freezing point.

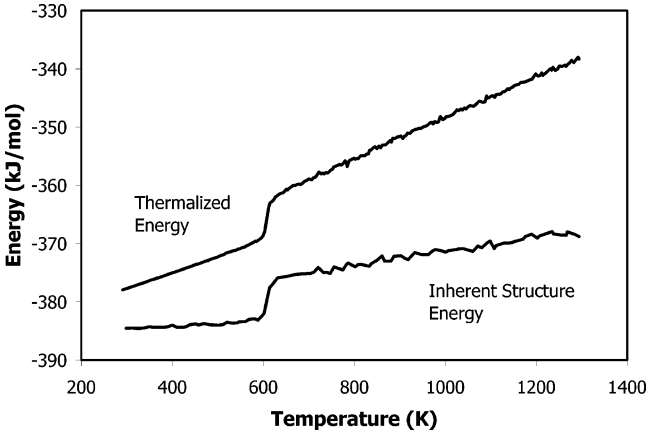

Figure 1. Comparison of thermalized and inherent structure energies for a crystallizing system with 5% CsCl cooled at a rate of 1.67 K/ps under constant-pressure conditions.

Systems with 0, 1, 5, 8, 10, and 15 mol % CsCl were cooled with a nominally constant rate of 1.67 K/ps. The initial configuration for cooling runs in each concentration was derived from the high-temperature (i.e., 1300 or 1700K) configuration of the previous run equilibrated for 50 000 or 20 000 time steps, respectively. For the constant-pressure runs, a pressure of 100 kPa was maintained with the Andersen barostat. For most runs, configurations were saved every 6 ps ($\sim$10 K). These configurations were then quenched to their inherent structures.

A steepest descent algorithm was used to quench the thermalized configurations.[25] This simply consisted of performing the Verlet integration to update positions with the velocity of each particle zeroed at the beginning of each time step. Such quenches were carried out at constant volume using increasing time steps (10, 20, and 25 fs or 5, 10, and 15 fs) until no further systematic decrease in energy was observed followed by a smaller time step (2 fs) in order to refine the inherent structure. The energy of the quenched system is shown in Figure 1, for a crystallizing system with 5% CsCl, as a function of the temperature of the thermalized system and compared to the thermalized energy of the system from which it was derived.

2.3. Crystallization versus Glass Formation. This system displays additional interesting behavior on the basis of the fact that pure NaCl always crystallizes in our simulations, even at the highest cooling rates. Figure 2 shows the dependence of supercooling in pure NaCl on the cooling rate under constant pressure. Melting is observed close to the experimentally determined value (1074 K). Faster cooling rates result in stronger supercooling before crystallization occurs. In our simulations, crystallization can occur at very low temperatures, showing that this process seems to require virtually no thermal activation. Accordingly, we surmise that the potential energy landscape for pure NaCl is rather featureless, much like the surface of a funnel leading to the deepest energy minimum of the crystalline state. To achieve glass formation, we need to add a small amount of CsCl. Due to the cation size mismatch, NaCl and CsCl are not miscible in the solid state. Rapid cooling of NaCl−CsCl mixtures therefore produces homogeneous glasses for as long

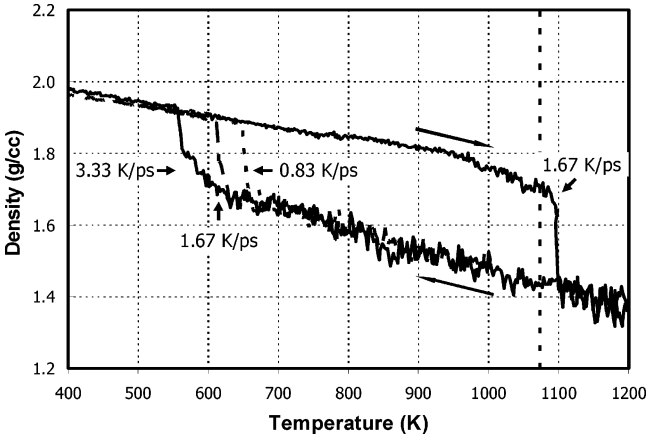

Figure 2. Dependence of crystallization temperature on the cooling rate for pure NaCl at constant pressure.

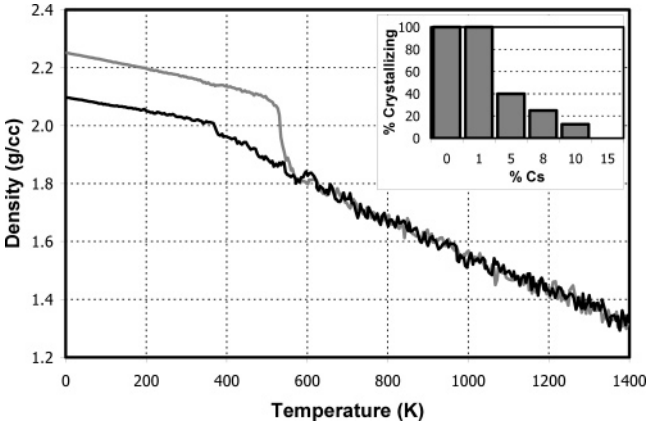

Figure 3. Density vs temperature for 0.95NaCl−0.05CsCl cooled at constant pressure. Inset: effect of CsCl concentration on crystallization probability.

as phase separation, which would normally occur at experimental time scales, is avoided.

The addition of CsCl seems to introduce additional energy states into the landscape that are blocked from the rest of the funnel surface by energy barriers. The number of extra states and the severity of disturbance of the original potential energy surface depends on the amount of CsCl added to the system. Hence, by gradually increasing this amount, we can tune the probability of crystallization versus glass formation and eventually reach the crossover from one to the other behavior. By increasingly frustrating the system, we can achieve glass formation without changing the time allowed for the atoms in the system to relax. Therefore, any differences between the behaviors of crystallizing and glass-forming systems may be identified on the basis of structure and largely independent of kinetic factors.

Figure 3 shows density traces for two systems with 5% CsCl. In one case, the system crystallizes, and in the other, it forms a glass. We have determined the crystallization probabilities for several concentrations of CsCl by cooling on average five systems of each concentration and counting the number of crystallizing systems. This probability is shown in the inset in Figure 3 versus CsCl concentration. For example, the probability for the 5% CsCl system to crystallize is ∼40% at this particular cooling rate of 1.67 K/ps. Of the 24 systems that we investigated in total, not counting pure NaCl, one-third crystallized. To explore why crystallization occurs in some cases and glass formation in others, we analyzed different geometric measures of the structures of these systems. In particular, it is useful to compare these measures for the supercooled liquids just above the crystallization or glass transition temperatures with those at lower temperatures when the transitions have occurred. Parts a and b of Figure 4 show the all-atom pair correlation functions, $g(r)$, for a crystallizing system and a glass-forming system containing a mixture with 10% CsCl at about 400 and 550 K, respectively. Clearly, there are significant differences in the high- and low-temperature distribution functions for the crystallizing system due to the formation of the ordered crystal structure. The glass-forming system's high- and low-temperature $g(r)$'s are, however, virtually indistinguishable, indicating the absence of long-range order and a truly amorphous structure. These plots may be used for calibration purposes, to judge what detail can be extracted by this correlation function. Obviously, the $g(r)$ of an ordered crystal has much better defined peaks than that of a glass, but even for the crystalline system, thermal disorder causes significant broadening in the peaks and some features, like the split in the third-neighbor peak, are difficult to discern.

In the liquid state, the total $g(r)$ for the glass-forming and crystallizing systems are indistinguishable within procedural accuracy, and so are the respective Na−Na, Na−Cs, Na−Cl, Cs−Cl, and Cl−Cl partial correlation functions. The most significant differences between the glass-forming and crystallizing systems are revealed by the Cs−Cs partial pair correlation function. Parts c and d of Figure 4 show this function for the same systems below and above the transition temperatures, respectively. For the crystallized system (Figure 4c), the first coordination peak is larger and is located at a slightly smaller Cs−Cs distance than that in the glass-forming one. In the CsCl crystalline structure, this peak would be located at 0.412 nm. In addition, there is a pronounced shoulder toward larger r in this peak and the next peak occurs at a smaller distance than the second peak in the $g_{Cs-Cs}(r)$ of the glass-forming system. While above the transition temperature the structure of both crystallizing and glass-forming systems are still in flux, the distinguishing features in the arrangement of Cs atoms are already partially developed (Figure 4d), indicating that the glass forming and crystallizing liquids may already be trapped in different metastable regions of the energy landscape and unable to explore the entire landscape at this temperature. The analysis of partial correlation functions suggest that, in the crystallizing system, the Cs atoms are more tightly clustered, possibly arranged in a configuration compatible with a rocksalt form of CsCl.

To corroborate this perception, we performed Voronoi tessellations on the inherent structures of the above configurations. One way to carry out this analysis is to include all atoms in the configuration and determine the volume that can be attributed to a given atom as delineated by the planes that intersect the middle of the connecting lines with each neighbor at a right angle. In Figure 5a and b, we show the results of this analysis, which was performed using the program HULL with periodic boundary conditions applied to the system.[26−28] In these graphs, we plot histograms showing the distribution of volumes occupied by atoms of a given species, normalized with respect to the total volume of the simulation box. Somewhat broader distributions are observed for systems that form glasses, while for crystallizing configurations the distributions are more asymmetric and rise sharply at low-volume values. We observe a slightly smaller average volume per atom for crystallizing systems. However, these distributions shed little light on the reason one configuration crystallizes and another forms a glass.

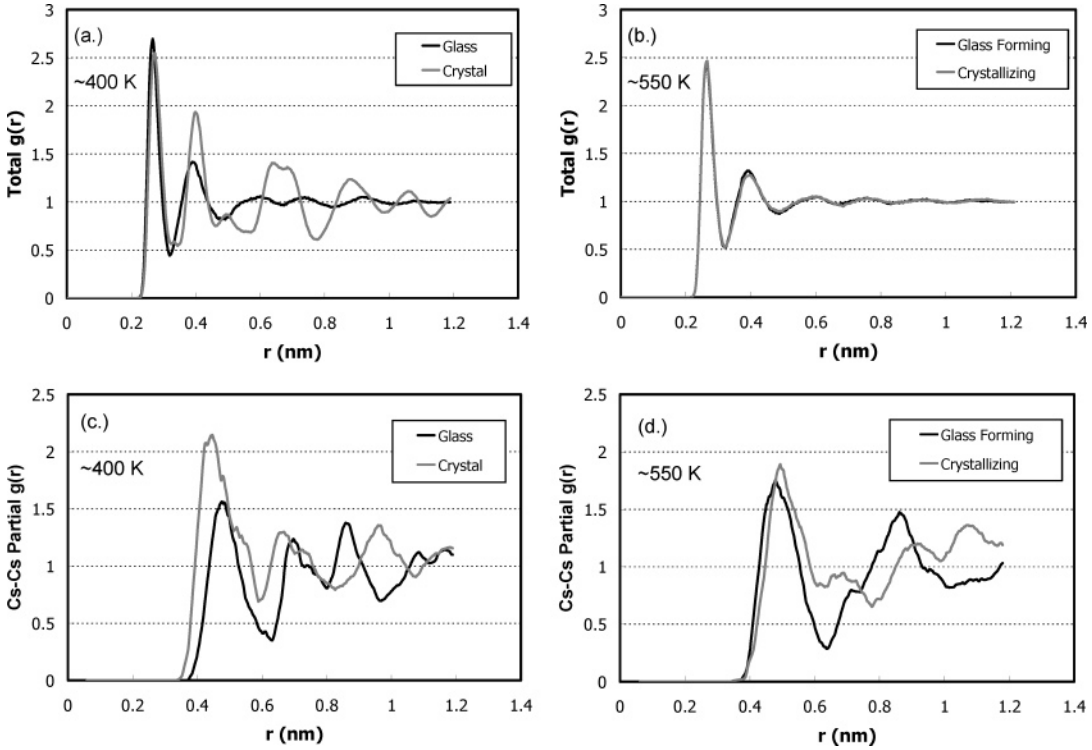

Figure 4. (a and b) All-atom pair correlation functions, $g(r)$, for systems with 10% Cs doping that form glass and crystals at ~400 K and ~550 K, respectively. (c and d) Cs−Cs partial $g(r)$ slightly below, ~400 K, and slightly above the transition temperature, ~550 K, respectively.

Alternatively, one can limit the tessellation construct to a single species, ignoring the volume occupied by the other species. Here again, the most revealing differences are found for the Cs-specific tessellations (see Figure 5c). These show a broader distribution of volumes for crystallizing systems than for glass formers. In particular, the Voronoi volume distribution for the crystalline configuration shows a lobe at small volumes (between 1.8 and 2.7%), which is entirely missing for the glassy configuration. Small volumes in the Cs-specific tessellation mean close coordination of Cs by Cs. This confirms the conclusions we drew from the pair correlation function analysis, namely, that crystallization is favored if Cs-rich clusters develop in the system. Essentially, Cs has to segregate into nanosized domains in order to develop local structures that are compatible with the NaCl lattice. Conversely, glass formation is favored by a more uniform distribution of Cs across the system. The same observation is also made when comparing a glass-forming system and a crystallizing system with 5% CsCl, indicating that such an effect likely occurs throughout the composition range where both crystallization and glass formation are possible.

3. Results and Discussion

In this section, we discuss the glass-forming behavior of NaCl−CsCl mixtures in the context of the energy landscape the systems explore upon cooling. In particular, we consider the structural evolution along isobars, which, contrary to constant-volume cooling where the energy landscape is fixed, implies an evolving landscape topology. For the most part, we concentrate on systems containing 10% CsCl, so that we can examine its glass-forming behavior in direct reference to a crystalline ground state. For comparison, we also cooled one configuration under constant-volume conditions. The density of this system is 2.15 g/cm^3, which is the equilibrium density at 245 K for the glassy systems with 10% CsCl, cooled isobarically at 100 kPa. Figure 6 shows the average inherent structure energies for this isochoric cooling process as a function of the equilibration temperature. We observe the ubiquitous sigmoidal profile, similar to that observed for Lennard-Jones systems.[13] The shape of this curve has been described as a hallmark for glass-forming behavior. Here, we fit the data using the expression

$$e_{IS} = e_0[1 + e^{-\Delta H(T_c - T)/k_B T T_c}]^{-1} \quad (2)$$

where e_0, ΔH, and T_c are parameters which describe the Boltzmann statistics for occupation of a two-level system.[29] Note that the use of this particular expression is not intended as a means for interpretation of the data but merely for convenience sake, as the fit is needed later for comparison purposes. The changeover from a high- to low-temperature plateau has been associated with the fact that below a certain temperature the system is no longer capable of exploring the entire potential energy surface, for lack of sufficient activation energy. The system gets trapped in the basins of local energy minima, which correspond to mechanically stable but noncrystalline configurations. Hence, a requisite for a good glass former is the existence of a large number of possible configurations to settle into with relatively low-lying potential energy levels, that is, an inherent structure energy distribution that is broader than that of simple liquids prone to crystallization.[13]

During isobaric cooling, the volume of the system changes with temperature so as to maintain approximately zero pressure, and consequently, the topology of the energy landscape changes. One can think of this as the landscape hypersurface having gained one additional dimension, or, considering only scaled atomic coordinates as possible degrees of freedom, the shape of this hypersurface morphing while the system progresses along its nonsteady contours. One might therefore expect that the system will follow a significantly different path on its way to a glassy state. The profiles of the inherent structure energies for cooling at constant pressure are shown in Figure 7a. The

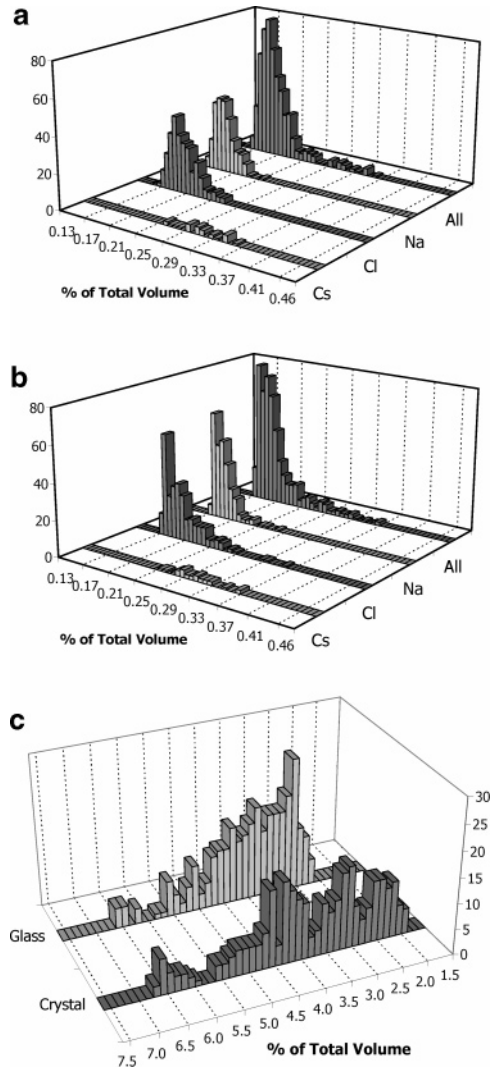

Figure 5. Histograms of the Voronoi volumes for 0.9NaCl−0.1CsCl inherent structures originating from configurations at ∼400 K considering (a) all atoms for a glass-forming system, (b) all atoms for a crystallizing system, and (c) only Cs atoms for both. The volumes are expressed as percentages of the total system volume. Part c has been rotated so as to more clearly show the differences in the distributions at low and high volumes.

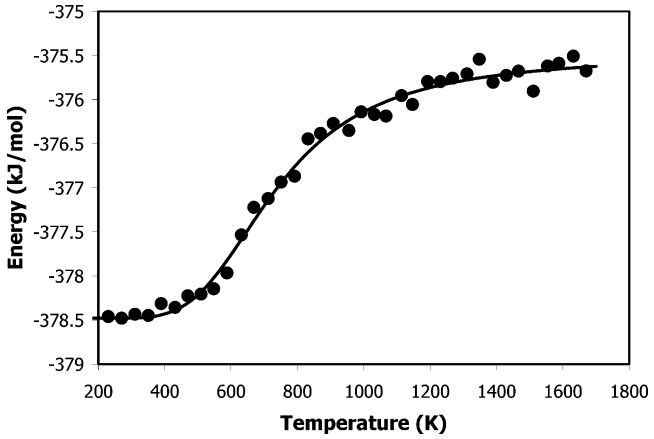

Figure 6. Inherent structure energies for a glass-forming system with 10% CsCl cooled at constant volume. The line represents the best fit of the data using eq 2.

most prominent feature in these data is a continuous increase of this energy with temperature. This is to be expected, since

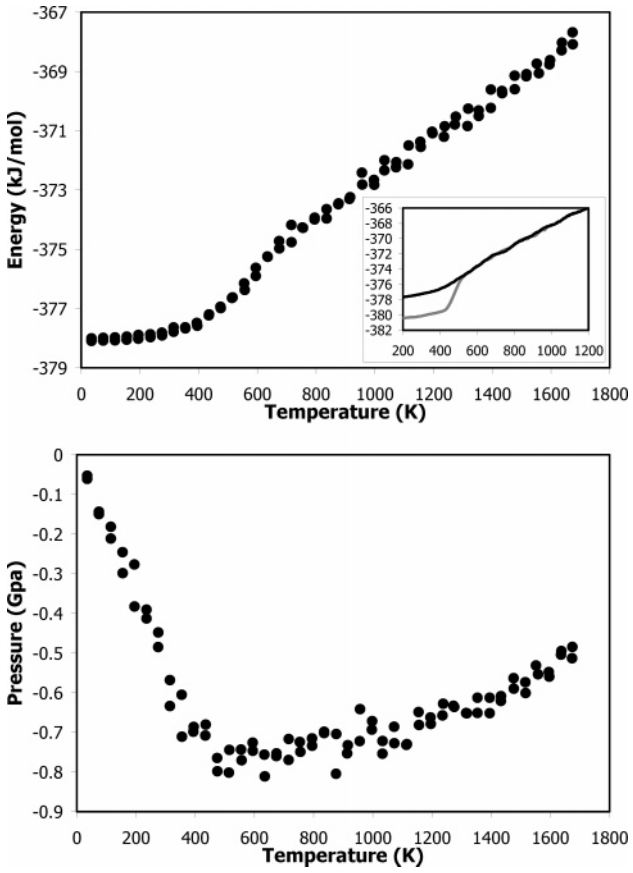

Figure 7. (a) Inherent structure energies for a 10% CsCl system cooled at constant pressure (100 kPa). The inset shows a close up comparison of the transition region for glass-forming and crystallizing systems that have slightly different thermal histories than those in the main panel. (b) Pressure−temperature relation of the quenched structures corresponding to the data in the main panel of part a.

inherent structures are maintained at the same volume as the thermalized system. Preventing the configuration from contracting during the inherent structure quench, as its thermal expansion coefficient would prescribe, will result in a hydrostatic tensile stress. This is equivalent to taking the inherent structure configuration at its equilibrium density at 0 K and expanding it isotropically, that is, imparting volume work. It is this volume work that is responsible for the predominant increase of the inherent structure energy with temperature.

The thermal expansion of liquids has previously been considered from an inherent structure point of view.[30] It has been shown that for some simple liquid models with purely repulsive potentials the thermal expansion can be accounted for by vibrational effects within the energy basins corresponding to the inherent structures, and the effect of the change in population of the basins is negligible. It has also been suggested that this is not the case in good glass formers based in part on the abrupt change in the inherent structure energies with temperature in the supercooled liquid regime above the glass transition under constant-volume conditions. This indicates a strong dependence of basin population on temperature (at least over this narrow temperature range).

Closer inspection of the data in Figure 7a reveals a discontinuity at around 700 K and more pronounced curvature below that temperature, possibly a second change in slope between 400 and 500 K. These features are barely perceptible, and the proposition that there is in fact a changeover between two temperature regimes, one above 700 K and the other below 400

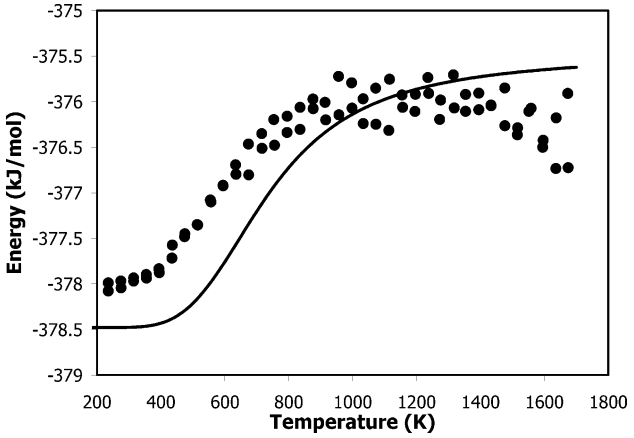

Figure 8. Inherent structure energies of a 10% CsCl system cooled at constant pressure corrected for pressure−volume work and the fit to the constant-volume inherent structure energies of Figure 6.

K, is only substantiated as a result of the correcting data treatment described below. As confirmed by the corresponding density versus temperature behavior, we can approximately identify the low-temperature change in slope with the simulated glass transition. The changeover region is magnified in the inset of Figure 7a for a system with a somewhat different thermal history, along with a trace of the inherent structure energies of a crystallizing system, to show that crystallization takes place well below the first change in slope upon cooling and just above the glass transition. This means that a supercooled liquid in the NaCl−CsCl system always experiences an initial slowing in structural relaxation, regardless of whether it finally crystallizes or forms a glass.

The question then arises whether there is any connection between this changeover and the sigmoidal energy drop observed during isochoric cooling. We therefore attempt to reconcile the two data sets by subtracting the pressure−volume work associated with the thermal expansion of the isobarically cooled glass former, according to

$$E_{\text{corrected}} = E_{\text{measured}} + \int_{V(T_0)}^{V(T)} P \, \mathrm{d}V \qquad (3)$$

where $V(T_0)$ and $V(T)$ represent the volumes of the final configuration resulting from cooling (i.e., at the lowest temperature, T_0) and the configuration of interest (at the variable temperature, T), respectively. Note that $V(T_0)$ is essentially the same volume as that of the isochorically cooled system in Figure 6. The pressures needed for this integration are those of the inherent structures derived from the constant-pressure cooling runs. These pressures are plotted versus the temperature of the parent configurations in Figure 7b. The corrected inherent structure energies versus equilibration temperature are shown in Figure 8. Indeed, we recover the sigmoidal shape, very similar to that of the inherent structure energies from the constant-volume cooling. The curve fitting the data in Figure 6 has been superimposed in Figure 8 as a guide for comparison. Accordingly, the inflection point in the corrected inherent structure energy data occurs at a somewhat lower temperature than that for the constant-volume case. This is not surprising, considering that the evolving energy landscape during isobaric cooling likely results in a different relaxation path compared to isochoric cooling and considering the high pressure that the system under isochoric conditions experiences at elevated temperature, which is likely to drive the glass transition to a higher temperature. Surprisingly, the difference in energy levels between glass and liquid are very comparable for isobaric and isochoric cooling.

On the basis of this comparison, it would appear that a relatively simple correction by pressure−volume work imparted during thermal expansion allows one to convert isobaric inherent structure energies into isochoric ones. This is, however, a conclusion that needs to be considered with caution, particularly because the inherent structures obtained from isobaric cooling transition from homogeneous at low equilibration temperatures to heterogeneous at higher temperatures.[31] Note that, for reasons explained above, the inherent structure pressures shown in Figure 7b are always negative. However, a minimum pressure (maximum tensile stress) is reached around an equilibration temperature of 500 K. This corresponds to the tensile limit of this system at 0 K. At this magnitude of negative pressure, the inherent structure is expected to rupture, and above the minimum on the equilibration temperature scale, that is, at lower densities, the structure is expected to separate into fragments interlaced with void space, hence the term heterogeneous. This is analogous to the shredding point described for Lennard-Jones systems[3,13,32] (e.g., see Figure 3 of ref 13), in which it has been demonstrated that the inherent structures of simple liquids develop a certain degree of porosity as a result of a process similar to spinodal decomposition with a dense phase and a void volume rather than two phases.[33] In these studies, the location of the shredding point (or Sastry density) was determined by isothermally expanding the structures.

With this in mind, it is more surprising to find that the isobaric and isochoric inherent structure energies can be converted into one another via a simple pressure−volume work correction. One might expect that such an operation would only be valid when performed within the stability range of a homogeneous phase and not across a point of conversion between homogeneous and heterogeneous phase character. This may indicate that the inherent structures beyond the tensile limit are not truly heterogeneous, in a sense that separate phases have developed through irreversible internal reconstruction (at least for the dense phase in this case), with well-defined interfaces between them. It was also proposed earlier[33] that the minimum in the equation of state of a liquid's energy landscape represents a lower bound in terms of density possible for glass formation. On the basis of our simulation results, we can further refine this observation to state that, on the equilibration temperature scale and within procedural error, the minimum pressure for the inherent structures derived from isobarically cooled configurations coincides with the glass transition temperature. This would imply a fundamental difference between glass and liquid, for our system, which is revealed by their inherent structures. Below the glass transition temperature, cohesive forces exist uniformly in every part of the structure. Above that temperature, the instantaneous cohesive forces are inhomogeneous and distinct void spaces exist in mechanical equilibrium within a fluctuating network of dense patches. For the parent configurations at temperature, this means that the free volume in the glass is the residue of a kinetically limited relaxation because, if it were not for the thermal motion, the structure would strive toward the densest possible packing. Conversely, in the liquid, free volume is accommodated in thermodynamic equilibrium and removal of the thermal energy would not cause this free volume to fully collapse. Additional studies are needed to address the effect of pressure on this glass transition-tensile limit correspondence and test for its existence in substances with different properties, e.g. materials with negative thermal expansion near the glass transition.

4. Conclusions

We have simulated inherent structures for various compositions of the NaCl−CsCl pseudobinary system. For a small range of NaCl-rich compositions, we can achieve both glass formation and crystallization at the same composition. This depends on the arrangement of Cs cations in the configuration. Crystallization is apparently favored when Cs segregates into nanosized domains.

We have examined systems that were cooled under both constant-volume and constant-pressure conditions. In both cases, systems undergo a changeover between liquid and glassy behavior that takes place over a span of several hundred kelvins. For systems cooled at constant volume, this changeover is apparent in the sigmoidal shape of the inherent structure energy versus temperature plot. Constant-pressure cooling yields inherent structure energies that exhibit a strong linear bias in their temperature dependence and more subtle changes of slope at the top and bottom of the changeover region. The change of slope at the lower temperature corresponds to the glass transition. By correcting for the pressure−volume work that the inherent structures of constant-pressure systems are subject to, the inherent structure energies for both constant-pressure and constant-volume cooling can be reconciled within good qualitative agreement.

The pressure of these inherent structures for systems cooled at constant pressure plotted versus the equilibration temperature shows a distinct minimum that approximately coincides with the glass transition. This pressure minimum (or maximum tensile stress) corresponds to the shredding point of the inherent structure and separates two fundamentally different regimes for the prevailing cohesive forces in the system. In the glass, cohesive forces act uniformly between neighboring structural elements, whereas, in the liquid, these forces are spatially and temporally non-uniform, so as to sustain a finite amount of void space in thermodynamic equilibrium.

Acknowledgment. J.W.P. was partially supported by the Fannie and John Hertz Foundation Fellowship.

References and Notes

(1) Stillinger, F. H.; Weber, T. A. *Phys. Rev. A* **1983**, *28*, 2408.
(2) Debenedetti, P. G.; Stillinger, F. H. *Nature* **2001**, *410*, 259.
(3) La Viollete, R. A. *Phys. Rev. B* **1989**, *40*, 9952.
(4) Sciortino, F.; Kob, W.; Tartaglia, P. *Phys. Rev. Lett.* **1999**, *83*, 3214.
(5) Scala, A.; Angelani, L.; Leonardo, R. D.; Ruocco, G.; Sciortino, F. *Philos. Mag. B* **2002**, *82*, 151.
(6) Sastry, S.; Debenedetti, P. G.; Stillinger, F. H. *Nature* **1998**, *393*, 554.
(7) Jonsson, H.; Andersen, H. C. *Phys. Rev. Lett.* **1988**, *60*, 2295.
(8) Saika-Voivod, I.; Sciortino, F.; Poole, P. H. *Phys. Rev. E* **2004**, *69*, No. 041503.
(9) Della Valle, R. G.; Andersen, H. C. *J. Chem. Phys.* **1992**, *97*, 2682.
(10) Stillinger, F. H. *J. Phys. Chem. B* **1998**, *102*, 2807.
(11) Doliwa, B.; Heuer, A. *Phys. Rev. Lett.* **2003**, *91*, No. 235501.
(12) Vogel, M.; Doliwa, B.; Heuer, A.; Glotzer, S. C. *J. Chem. Phys.* **2004**, *120*, 4404.
(13) Debenedetti, P. G.; Stillinger, F. H.; Truskett, T. M.; Roberts, C. J. *J. Phys. Chem. B* **1999**, *103*, 7390.
(14) Middleton, T. F.; Wales, D. J. *J. Chem. Phys.* **2003**, *118*, 4583.
(15) Angell, C. A.; Borick, S. *J. Non-Cryst. Solids* **2002**, *307*, 393.
(16) Giovambattista, N.; Mazza, M. G.; Buldyrev, S. V.; Starr, F. W.; Stanley, H. E. *J. Phys. Chem. B* **2004**, *108*, 6655.
(17) Roberts, C. J.; Debenedetti, P. G.; Stillinger, F. H. *J. Phys. Chem. B* **1999**, *103*, 10258.
(18) Dellavalle, R. G.; Andersen, H. C. *J. Chem. Phys.* **1992**, *97*, 2682.
(19) Poole, P. H. *Curr. Opin. Solid State Mater. Sci.* **1998**, *3*, 391.
(20) La Violette, R. A.; Budzien, J. L.; Stillinger, F. H. *J. Chem. Phys.* **2000**, *112*, 8072.
(21) Wevers, M. A. C.; Schon, J. C.; Jansen, M. *J. Phys. A* **2001**, *34*, 4041.
(22) Fumi, F. G.; Tosi, M. P. *J. Phys. Chem. Solids* **1964**, *25*, 31.
(23) Reardon, B. J.; Kieffer, J. *Philos. Mag. B* **1998**, *77*, 907.
(24) Reardon, B. J. Dynamics in Molecular Structures−Instabilities, Transport, and Transformations. Ph.D. Thesis, University of Illinois, 1997.
(25) Leach, A. R. *Molecular Modelling: Principles and Applications*, 2nd ed.; Prentice Hall: New York, 2001.
(26) Clarkson, K. *HULL*. http://cm.bell-labs.com/netlib/voronoi/hull.html.
(27) Clarkson, K. L. Safe and effective determinant evaluation. Proceedings of the 31st IEEE Symposium on Foundations of Computer Science, Pittsburgh, PA, 1992.
(28) Clarkson, K. L.; Mehlhorn, K.; Seidel, R. *Comput. Geometry-Theory Appl.* **1993**, *3*, 185.
(29) Kieffer, J. *J. Phys. Chem. B* **1999**, *103*, 4153.
(30) Stillinger, F. H.; Debenedetti, P. G. *J. Phys. Chem. B* **1999**, *103*, 4052.
(31) Stillinger, F. H. *Phys. Rev. E* **2001**, *63*, No. 011110.
(32) Hernandez-Rojas, J.; Wales, D. J. *Phys. Rev. B* **2003**, *68*, No. 144202.
(33) Sastry, S.; Debenedetti, P. G.; Stillinger, F. H. *Phys. Rev. E* **1997**, *56*, 5533.